

Kinematic structure of the atmosphere and envelope of the post-AGB star HD 56126

Valentina Klochkova & Eugenij Chentsov

Special Astrophysical Observatory RAS, Nizhnij Arkhyz, Russia

October 29, 2018

Abstract We present results of an analysis of the optical spectrum of the post-AGB star HD 56126 (IRAS 07134 + 1005) based on observations made with the echelle spectrographs of the 6-m telescope with spectral resolutions of $R = 25000$ and 60000 at $4012\text{--}8790 \text{ \AA}$. The profiles of strongest lines (HI; FeII, YII, BaII absorptions, etc.) formed in the expanding atmosphere at the base of the stellar wind have complex and variable shapes. To study the kinematics of the atmosphere, the velocities of individual features in these profiles must be measured. Differential line shifts of up to $V_r = 15\div 30 \text{ km/s}$ have been detected from the lines of metals and molecular features. The star's atmosphere simultaneously contains both expanding layers and layers falling onto the star. A comparison of the data for different times demonstrates that both the radial velocity and the velocity pattern in whole are variable. The position of the molecular spectrum is stable, implying stability of the expansion velocity of the circumstellar envelope around HD 56126 detected in observations in the C_2 and NaI lines.

1. Introduction

We studied the kinematic parameters of the atmosphere of the star HD 56126 (SAO 96709), which belongs to the asymptotic giant branch (the post-AGB stage). In this short evolution stage, stars are in the process of their transition from the AGB to becoming a planetary nebula; for this reason, they are generally known as proto-planetary nebulae (PPNe). In the Hertzsprung–Russell diagram, post-AGB stars evolve toward the left from the AGB, maintaining nearly constant luminosity while becoming hotter. As descendants of AGB stars, these objects can be used to trace variations in the physical conditions and chemical parameters of the stellar material due to changes in the sources of energy release in the stellar interior, the ejection of the envelope, and mixing.

HD 56126 is the optical component of the IR source IRAS 07134+1005, which has a double peaked spectral energy distribution (SED), typical for PPNe. In addition to this anomalous SED, associated with the circumstellar dust envelope, the star also displays other characteristics of this type of object [1]: the optical component of the PPN is a F5 Iab supergiant outside the galactic plane ($b=+9^m 99$); the central star is surrounded by an extended nebula whose angular size exceeds $4''$, according to Hubble Space Telescope observations [2] (the largest known for this type of PPN); and the optical spectrum displays $H\alpha$ emission and absorption with a variable line profile [3]. In addition to these general PPN characteristics noted by Kwok [1], subsequent studies of HD 56126 and the associated IR source revealed several important peculiarities expected for this evolution stage: a large excess of carbon and s -process elements [4] and an emission feature at $\lambda = 21 \mu$ in the IR-spectrum.

In the small subgroup of PPN having this emission, the presence of this 21μ feature was found to correlate with observational manifestations of the products of nucleosynthesis (the excess of carbon

Table 1. Moments of observations and values of heliocentric radial velocity V_r measured. Column 4 contains V_r values averaged over weak lines (with depths R_λ close to the continuum level, $R_\lambda \rightarrow 0$). Velocities corresponding to the positions of the strongest components are presented for FeII(42), H α , and D2NaI, with values determined from the weakest components given in parantheses. The two velocities in italics in column 5 are determined from the IR–oxygen triplet OI 7773 Å. Uncertain values are marked by a colon.

Date	Spectro- graph	$\Delta\lambda$ Å	V_r							intestellar		
			$R_\lambda \rightarrow 0$	FeII	H β	H α	D NaI	C ₂				
1	2	3	4	5	6	7	8	9	10	11	12	
12.01.93	Lynx	5560–8790	88.8	<i>91</i>		78 (100:)	77	79:				
10.03.93	Lynx	5560–8790	89.0	<i>93</i>		71 (43:)	75:	76:				
04.03.99	Lynx	5050–6640	85.9	77		76 (43:)	78	77.1				
20.11.02	NES	4560–5995	89.6	95 (80:)	89		74.9 (89)	77.2	12.0	23.5	30.8	
21.02.03	NES	5150–6660	88.8	96:		88 (112:)	75.6 (89)	77.1	12	24	31	
12.04.03	NES	5270–6760	88.4			82 (103:)	75.4 (89:)		13	23	30.5	
14.11.03	NES	4518–6000	85.3	96 (86:)	97		75.0 (87:)	76.9	12.5			
10.01.04	NES	5270–6760	86.7			54: (78:)	75.6 (86:)		13.0	23.5	31	
09.03.04	NES	5275–6767	89.8			58 (74:)	76.1 (89)		13	24	31	
12.11.05	NES	4010–5460	82.5	97 (77:)	98			77.5				

and heavy metals in the outer layers of the atmosphere) [5, 6]. Thus, HD 56126 displays all the properties expected for a post-AGB object, indicating the importance of detailed studies of its optical spectrum with high spectral resolution in a broad wavelength range. Fortunately, HD 56126 is fairly bright ($B = 9^m 11$, $V = 8.27m$), making it the most convenient carbon enriched PPN star for high resolution spectroscopy.

The main moments of our study are spectral features identification and comparison the spectra of HD 56126 and the standard α Per (Sp = F5 Iab); search for profile variability for spectral features; analyses the radial velocities V_r to search for differential shifts; and studying the variability of the radial velocity. In Section 2, we briefly describe the techniques used for the observations, processing, and analysis of the spectral data. The main conclusions concerning the spectrum of the star are presented in Section 3.1, while Sections 3.2 and 3.3 present our radial velocity measurements derived using various features of the spectrum, and discuss the temporal behavior of the radial-velocity pattern. Our results are summarized in Section 4.

2. Observations and reduction of the spectra

We observed HD 56126 and α Per with the 6-meter telescope of the Special Astrophysical Observatory. All the spectra were obtained at the Nasmyth focus with the NES [7, 8] and Lynx [9, 10] echelle spectrographs. In combination with a 2048×2048 CCD and the image cutter [11], NES provides a spectral resolution of $R = 60000$. The Lynx spectrograph used with a 1K×1K CCD yields $R = 25000$. The Table presents the observing dates and wavelength regions detected. The spectral data were extracted from two-dimension echelle-spectra using the ECHELLE context in the MIDAS package modified to take into account specific features of the echelle frames obtained with these spectrographs (see [12] for details). Cosmic-ray traces were removed via median averaging of pairs of consecutive spectra. The wavelength calibration was carried out using spectra of a hollow cathode Th-Ar lamp.

The further processing, including photometric and position measurements, was performed using the DECH20 code [13], which makes it possible to find the positions of spectral features by overlapping their direct and mirrored profiles. To increase the accuracy of the radial-velocity measurement, the least blended lines in the observed and corresponding synthetic spectra were compared.

In each spectrogram, the positional zero point was determined in the standard way, via calibration using the positions of ionospheric night-sky emission lines and telluric absorptions in the star spectrum. The accuracy of the velocity measured from **one line** in the spectra obtained with the NES and Lynx spectrographs is about 1.0 and 1.5 km/s, respectively.

3. Results

A list of the lines we identified in the spectrum of HD 56126 is presented at <http://www.sao.ru/hq/ssl/HD56126-Atlas/Atlas.html>. This contains only a partial set of the lines for which the depths R and heliocentric radial velocities V_r were measured. Let us consider in more detail the peculiarities of the spectrum.

3.1. Peculiarities of the spectrum of HD 56126

Interstellar features. Comparing our data with those obtained by other authors, we tested the coincidence of the radial-velocity zero points using interstellar and circumstellar lines. Figure 1 presents the D2 NaI line profiles; both here and in the Table, to display the fine structure of the lines, we consider only spectra obtained with our maximum resolution, $R = 60000$. As a result, five components of the D2 NaI line can be distinguished. Three blue-shifted interstellar components of the D2 line in the spectrum of HD 56126, clearly seen in Fig. 1, yield the same V_r values within the errors (columns 10–12 in the Table, with the averaged values $V_r = 12.6, 23.6,$ and 30.9 km/s). The stability of these values confirms that these three components are formed in the interstellar medium. The shift of the component of the D2 NaI line with $V_r = 75.8$ km/s is consistent with that of the Swan bands of the C_2 molecule (columns (8) and (9) of the Table), which indicates that this component is formed in the circumstellar medium. It is obvious that the longest-wavelength component, $V_r = 88.5$ km/s, is photospheric: its temporal behavior corresponds to that of other photospheric absorption features. Note that such a structure of the D NaI lines is consistent with the results obtained by Bakker et al. [14], who distinguished a weak component of the D2 NaI line with $\langle V_r \rangle = 44$ km/s, which is also seen in at least three of our spectra, yielding $\langle V_r \rangle = 46 \pm 1$ km/s. In addition, as we can see from Fig. 1, the blend of three blue-shifted components displays sharp boundaries, making it possible to reliably measure the velocity for the blend as a whole. The average value derived from our data, $V_r = 20.3 \pm 0.3$ km/s, coincides with that obtained by L'ebre et al. [16] from spectra with lower resolution: $V_r = 20 \pm 2$ km/s.

As was shown by Crawford and Barlow [15], when the C_2 and KI circumstellar features are observed with ultra-high resolution, they split into components spaced at about 1 km/s. These components yield the same set of velocities, but display different relative intensities. This may result in small systematic differences (also of the order of 1 km/s) in the velocities obtained for the atomic and molecular circumstellar lines at lower resolution. Our measurements do not indicate variations in these velocities, while the average values 77.2 ± 0.5 km/s for C_2 and 75.4 ± 0.3 km/s for NaI do not disagree systematically with those obtained by L'ebre et al. [16], Bakker et al. [14, 17], and Crawford and Barlow [15]: $77.3 \div 77.6$ km/s and $75.3 \div 76.8$ km/s for C_2 and NaI, KI, respectively.

H α line in the spectrum of HD 56126. The H α lines in the spectra of typical PPNe display complex (emission + absorption) variable profiles with asymmetrical core, P Cygni type profiles of various kinds from direct to inverted, profiles with asymmetrical emission wings, or profiles containing two emission components. A combination of such features is also frequently observed. As we can see from Fig. 2, the H α line in the spectrum of HD 56126 has both absorption and emission components, which are not seen in the spectrum of the normal supergiant α Per. Figure 2 also clearly shows the H α absorption wings, extending to values close to those for the H α wings in the spectrum of α Per. Figure 3, which presents only the central parts of the H α profiles for all our observations, demonstrates the profile variability from night to night.

Previously, based on their spectral monitoring of HD 56126, Oudmaijer and Bakker [3] concluded that the $H\alpha$ profile is strongly variable on timescales of two months. The analysis of the variability of the $H\alpha$ profile and the corresponding set of radial velocities using Fourier methods led L'ebre et al. [16] to conclude that there are complex, pulsation-driven, dynamical conditions in the atmosphere of HD 56126. The extensive set of high-quality spectral observations of HD 56126 over almost eight years of Barth'es et al. [18] indicated that, apart from $H\alpha$, the $H\beta$ line also varies. Analyzing the profile variability of both these hydrogen lines, these authors concluded that the observed variability does not display any periodicity that could be related to variations of the radial velocity and brightness of the star.

Swan bands. In addition to specific features of the HI line profiles, the peculiarity of PPNe optical spectra is also manifest in the presence of numerous molecular absorption features, along with lines characteristic of F–K supergiants. In the spectrum of HD 56126, with an effective temperature $T_{\text{eff}} = 7000$ K [4], the C_2 Swan absorption band system is observed, as well as the red CN system, first identified by Bakker et al. [14]. Later, molecular bands in the spectra of PPNe in another sample (including HD 56126), selected for the presence of the carbon-containing molecules C_2 , CN, and CH^+ in their envelopes, were studied in detail by Bakker et al. [17] using high-resolution spectra ($R = 50000$). Judging from the velocity corresponding to the position of these bands, the absorption molecular spectrum is formed in a restricted region of the envelope, close to the star [17].

Our spectra of HD 56126 contain several Swan bands. Figure 4 shows a spectral fragment with the head of the C_2 (0;0) band at 5165 \AA , and compares again the spectra of HD 56126 and the normal supergiant α Per. We present a detailed list of Swan band spectral features in the spectrum of HD 56126 and their intensities and corresponding radial velocities at <http://www.sao.ru/hq/ssl/HD56126-Atlas/Atlas.html>. The radial velocities derived from the Swan bands are analyzed in Section 3.2. Although Swan bands have been detected in emission in the spectra of several PPNe [5, 17], no signs of emission in these bands or in the D lines of NaI have been found in spectra of HD 56126 obtained in various years. This is consistent with the fairly simple elliptical shape of the nebula surrounding HD 56126.

Apparently, emission in the Swan bands or the D lines of NaI is observed only in the spectra of PPNe with bright circumstellar nebulae displaying pronounced asymmetry. This is confirmed by the spectroscopic results for IRAS 04296+3429 [19], IRAS 23304+6147 [20], AFGL 2688 [21], IRAS 08005–2356 [22], IRAS 20056+1834 [23, 24], and IRAS 20508+2011 [25]. As a rule, the HST images of these PPNe [2] display bipolar structure. We emphasize that most of these objects belong to Type 1 (PPNe with polarized optical radiation) according to the classification suggested by Trammell et al. [26].

Based on the parameters of the PPNe whose spectra we have studied, including HD 56126, we suggest that emission in the Swan bands and/or NaI D lines is observed in the spectra of PPNe (and related stars with envelopes) in which the outward propagation of the radiation of the central star is substantially hindered by absorption in the circumstellar dust envelope. Profiles of metal lines. Figures 5 and 6 show that the profiles of strong lines of metals in the spectrum of HD 56126 are not symmetrical. In addition, comparisons of spectra obtained on different nights indicate that, for the metallic lines formed in the expanding atmosphere of the star (at the base of the wind), the profile shape varies with both time and line intensity. Parthasarathy et al. [27] had already noted the asymmetry of the BaII 6141 \AA line profile in the HD 56126 spectrum. It cannot be ruled out that the variability of the profiles is due to splitting of the absorption lines into components whose positions and intensities are different at different times. High-spectral-resolution observations reveal the multicomponent structure of metal lines in the spectra of various types of variable stars, such as classical Cepheids (see, for example, [28]) or pulsating RV Tau [29] or W Vir type [30] stars, due to the presence of shocks (see also references below). The possibility for several shocks to coexist in the atmosphere of HD 56126 was shown by Barth'es et al. [18]. However, direct observation of the

splitting of metal lines in the spectrum of HD 56126 is complicated by broadening in the turbulent atmosphere of the supergiant.

3.2. Variability of the radial velocity pattern

Some of PPNe display variability of the radial velocity V_r with characteristic timescales of several hundred days, possibly providing evidence for binarity. Indeed, conclusive evidence for orbital motion has been obtained for several optically bright objects with IR-excesses. For example, the binarity of the high-latitude supergiants 89 Her [31, 32] and HR 4049 [33] has been proven, the corresponding orbit elements determined, and models of the systems proposed. Van Winckel et al. [34] showed that HR 4049, HD 44179, and HD 52961 are spectral binaries with orbital periods of about one to two years. Bakker et al. [35] studied the variability of complex emission-absorption profiles of the NaI D lines and $H\alpha$ for HR 4049 as functions of the orbital period using high resolution spectra. The individual components of these lines are formed either in the atmosphere of the primary, in the disk in which both binary components are submerged, or in the interstellar medium. The nature of the companions in suspected post-AGB binaries is still unknown, since there are no directly manifestations of their radiation in either the continuum or in spectral lines: all known post-AGB binaries are of type SB1. The companions could be very hot or very low luminosity main sequence objects; white dwarfs cannot be ruled out either, as in the case of BaII stars. The V_r variability in PPNe can also be complicated by differential motions in their extended atmospheres. A detailed analysis of V_r for selected bright PPNe using spectra with high spectral and temporal resolution reveals differences in the behavior of V_r determined from lines with different degrees of excitation, formed at different depths in the stellar atmosphere.

In the following Section, we point out such differences in the behavior of V_r for HD 56126. Variability of the radial velocity of HD 56126 was first suspected in [4], based on a comparison of published data with new data obtained on the 6-m telescope. In subsequent years, several authors studied this variability using high resolution spectroscopy. Oudmaijer and Bakker [14] used a very large collection of spectrograms with high time resolution and high S/N ratio, and concluded that there was V_r variability on timescales of several months in the interval $V_r = (84 \div 87) \pm 2$ km/s, with an absence of variations with characteristic timescales from minutes to hours.

L'ebre et al. [16] carried out detailed spectral monitoring of HD 56126. Applying a Fourier analysis to radial-velocity data together with data for the brightness variability, they concluded that the dynamical state of the atmosphere of HD 56126 and the pattern inherent to pulsating RV Tau variables were similar. They interpreted the $H\alpha$ variability as a result of shocks. Later, L'ebre et al. [36] studied the variability of the $H\alpha$ and $H\beta$ lines. Having augmented the spectral data and used also photometric observations, they determined the period of radial pulsations to be $P = 36^d.8$. Barth'es et al. [18] collected all reliable V_r measurements for HD 56126 (89 values obtained over eight years) and analyzed them with photometric data, revealing the presence of V_r variability with a half-amplitude of 2.7 km/s and the primary period $P = 36.8 \pm 0^d.2$. The photometric variability displays the same period, with a very low amplitude ($0^m.02$). They concluded that the star's variability differs substantially from the pulsations observed in RV Tau stars. With its fairly high temperature, HD 56126 has evolved further than the RV Tau stage. The variability of the brightness and radial velocity of HD 56126 may be due to first-overtone radial pulsations caused by shocks that generate complex, asynchronous motions in the upper hydrogen-rich layers of the star.

Our new V_r data for HD 56126 are summarized in the Table. Taking into account the large probability of differential shifts in the outer layers of the stellar atmosphere, we present here V_r values for individual lines and groups of lines. As we can see, the velocity variations are real, even when they are detected for weak absorption lines ($R_\lambda \rightarrow 0$). The positions of circumstellar features (the NaI D line and C_2 Swan band; see columns 8 and 9 of the Table) display good consistency. Their comparison with the data from column (4) yields an expansion velocity for the envelope

$V_{\text{exp}} \approx 11$ km/s. Note that the position of the primary $H\alpha$ component is not always consistent with the positions of the D NaI lines and Swan band, whereas the behavior of the $H\beta$ line is synchronized with the FeII(42) line. There are still no sufficient reasons to consider HD 56126 a binary; however, this cannot be conclusively ruled out, either. In this connection, it is worth noting the remark made by Barth'es et al. [18] concerning the weak trend of the star's radial velocity during their long-term observations. This trend may provide evidence for the presence of a second component in the system, with the orbital period exceeding 16 years. Our eight spectra, obtained at later dates, cannot clarify this situation. The variability of the velocities derived from extremely weak absorption lines, $V_r(R_\lambda \rightarrow 0)$, may indicate binarity of the star, but it may also be a manifestation of low-amplitude pulsations in circum-photospheric layers. Resolving the question of binarity for HD 56126 requires that the behavior of V_r be followed over several years, with one or two spectra obtained regularly each month.

3.3. Asymmetry of the profiles and differential shifts of the lines

When comparing our V_r values with those from other studies, we should bear in mind not only the different methods used, but also the spectroscopic peculiarity of the object, and the asymmetries of lines in the spectrum of HD 56126 (Figs. 5 and 6). The line profile shapes vary with both time and line intensity. Therefore, we will consider separately the data for the line cores in columns 4–8 of the Table (i.e., the lower parts of the absorption lines or the absorption components of the $H\alpha$ profiles; or sometimes, in the case of line splitting, individual components), and supplement these with the V_r estimates derived from the upper parts and edges of the profiles.

The large spectral interval recorded with the echelle spectrograph made it possible to study the differential radial-velocity patterns measured from lines with different intensities. For each of our spectra, we constructed the dependence $V_r(R)$ of the heliocentric radial velocity V_r measured in the absorption core on its central depth R . Figure 7 shows some of these dependences characteristic of HD 56126. The velocity of the center of mass of the star $V_{\text{sys}} = 86.1$ km/s [37] obtained from CO observations at millimeter wavelengths is marked by the horizontal dashed lines.

Most of the points in these graphs are confined within narrow, almost horizontal bands, in which the vertical scatter is determined by the uncertainties for individual lines. The right ends of the bands, corresponding to the strongest lines formed in the outer layers of the atmosphere, are sometimes turned upwards or downwards. For α Per, the $V_r(R)$ dependences are strictly horizontal over the total interval of line depths. When the C_2 molecular lines of HD 56126 appear in the studied spectral interval, the corresponding points also form short strips below the main bands, always at the same V_r level of about 77 km/s, as was noted above. In contrast, points corresponding to lines of atoms and ions can occur at, above, or below the level of V_{sys} (Fig. 7). Column 4 of the Table contains the average V_r values for the left edges of the main bands; i.e., the limiting values to which they tend when the central absorption intensities approach the continuum level (their depths $R_\lambda \rightarrow 0$).

Obviously, these can be considered the deepest layers of the atmosphere accessible to observations. Radial velocities derived from moderate-intensity absorption lines in the spectrum of HD 56126 are presented by L'ebre et al. [16] and Barth'es et al. [18]. These values were obtained from only two lines, BaII 5854 and Cl 6588 Å, but for several dozen observing epochs; the total range of variation of V_r is 81–93 km/s. Both of these lines lie on almost horizontal sections of our $V_r(R)$ dependences, to the left of the sharp breaks at $R \approx 60$ (Fig. 7c). The V_r values measured from our eight spectra that contain at least one of these two lines vary from 84 to 91 km/s, within the interval obtained by Barth'es et al. [18]. As we can see from Column 4 of the Table, the limits for the variations of the average velocities derived from the weakest absorption lines are somewhat lower: $82.5 \text{ km/s} < V_r(R_\lambda \rightarrow 0) < 89.8 \text{ km/s}$ (± 4 km/s relative to V_{sys}). The average values of our $V_r(R_\lambda \rightarrow 0)$ and for the two lines analyzed in [18] coincide within the errors (87.3 ± 0.7 and 87.7 ± 0.3 km/s).

The V_r values obtained from the stellar components of the NaI D lines (column 8 of the Table, the value in parentheses) are close to $V_r(R_\lambda \rightarrow 0)$, but less accurate.

Strong SrII and YII lines and other strong lines (with depths $R_\lambda \approx 60 - 70$; points on the $V_r(R)$ dependences to the left of the breaks) display large-amplitude time variations and a predominance of red shifts relative to the weakest absorption lines: $83 < V_r < 94$ km/s (-3 km/s, $+8$ km/s relative to V_{sys}). Both of these tendencies are even more pronounced in the FeII(42) and H α lines (columns 5 and 6 of the Table): $77 < V_r < 98$ km/s (-9 km/s and $+12$ km/s relative to V_{sys}). In three cases, the velocity could also be estimated from reliably detected blue-shifted components of the FeII(42) lines. The H α profile displays the highest variability, but for any profile presented in Fig. 3, an analogous profile can be found among those presented by L'ebvre et al. [16] and Barth'es et al. [18], in terms of both profile shape and the velocities derived from the absorption components. In our spectra, $V_r(\text{H}\alpha)$ (column 7 of the Table) varies from 54 to 88 km/s (-32 and $+2$ km/s, relative to V_{sys}) for the main (deeper) components and from 43 to 112 km/s (-43 and $+26$ km/s relative to V_{sys}) for the secondary components.

All the lines except those of hydrogen have the same type of asymmetry: their blue wing is extended more than the red, i.e., the velocity measured from the upper part of the profile (from the wings) is smaller than the velocity measured from the core. The blue shift of the wings relative to the core increases with line strength, either gradually or jump-like. In three of our spectra, obtained on November 20, 2002, March 9, 2004, and November 12, 2005, the absorption lines remain symmetrical up to $R_\lambda \approx 50$ (horizontal sections of $V_r(R)$ dependences in Fig. 7), but also display the above asymmetry for the deepest lines (Figs. 5 and 6). The FeII(42) absorption lines are asymmetrical for all our observing epochs (Fig. 6); on November 14, 2003 and November 12, 2005, the shift of their wings relative to their cores reaches -11 km/s. In contrast, in the spectrum obtained on March 4, 1999, the asymmetry is seen even in the weakest lines; in the interval $5 < R < 50$, as the lines deepen and their blue shifts grow, the difference between the V_r values measured from the wings and cores increases from -3 to -6 km/s, but the most blue-shifted FeII(42) absorption lines are again almost symmetrical (Figs. 6 and 7a). The wings of strong lines are less shifted relative to the weak lines than are their cores, and the velocities derived from the wings are closer to the center-of-mass velocity of the star (deviations from V_{sys} are from -10 to $+3$ km/s). We can see from Fig. 3 and the figures presented in [18] that both the blue the red slopes of the H α absorption component may be flatter (we are speaking here of the central part of the profile, rather than the broad photospheric wings).

Strong absorption lines in the spectrum of HD 56126 display fairly clear-cut boundaries, from which the velocities were also measured. These measurements show that the red boundary of the profile is substantially more stable than the blue. For the red boundaries of the strongest non-hydrogen lines, it is sufficient to indicate the average velocity, namely $V_r = 124 \pm 2$ km/s, while the velocity for the left boundaries ranges from 25 to 53 km/s. For H α , the same estimates yield $V_r = 133 \pm 5$ km/s and $10 \div 55$ km/s. Thus, the deviations from V_{sys} are $-33 \div -61$ km/s and $+38 \pm 2$ km/s in the former and $-31 \div -76$ km/s and $+47 \pm 5$ km/s in the latter case.

Summarising the measurements and analysis of the radial velocity pattern, we draw the following conclusions.

- Our data for the radial velocities of HD 56126 are fairly accurate (the systematic errors are below 1 km/s), making it possible to combine them with the most accurate data obtained previously.
- We have found substantial differential shifts for lines of different intensities within the same spectrum (up to 15 km/s for metallic lines, and up to 30 km/s for H α); these are the $V_r(R)$ dependences manifesting the V_r gradient. The time variability of the $V_r(R)$ dependences indicates that velocities should be measured using a large set of lines within an extended spectral interval.
- Both expanding matter and matter falling onto the star are seen in the stellar atmosphere.

- Data for extremely weak absorption lines are important ($V_r(R \rightarrow 0)$) for studies of the velocity pattern; the detected variability of these velocities, $82.5 < V_r(R \rightarrow 0) < 89.8$ km/s, may either represent low-amplitude pulsations in the circumphotospheric layers or indicate the star’s binarity.
- We have found complex and variable profiles of strongest lines (not only hydrogen, but also FeII, YII, BaII, and other absorption lines) formed in the expanding stellar atmosphere (at the base of the wind). Measurements for the velocities derived from individual features of these profiles are needed for kinematic studies.
- We have confirmed the stability of the expansion velocity for the circumstellar envelope of HD 56126, determined from the C₂ and D2 lines of NaI.
- High and ultra-high spectral resolution is needed to study, respectively, stellar and circumstellar lines in the spectrum of HD 56126 displaying complex structures.

4. Conclusions

Our high resolution spectra of HD 56126 have revealed variability of various line profiles: along with the previously known H α profile variability, the profiles of strongest lines (such as BaII, YII, and FeII) also proved to be variable. The broad spectral range encompassed by our spectra enabled us to measure radial velocities using spectral features that form at various depths in the stellar atmosphere and circumstellar envelope.

We were able to distinguish the C₂ absorption molecular bands (and their structure), as well as bands identified with diffuse interstellar bands. We found substantial differential shifts in lines of different intensities within the same spectrum, i.e., appreciable $V_r(R)$ dependences, as well as variation of these shifts with time. This indicates the need for velocity measurements based on a large set of lines in an extended spectral interval.

We conclude that both expanding layers and matter falling onto the star exist simultaneously in the stellar atmosphere. The position of the molecular spectrum is stable, indicating stability of the expansion velocity of the envelope.

Acknowledgements

This work was supported by the Russian Foundation for Basic Research (project code 05–07–90087), the program of basic research held by the Presidium of Russian Academy of Sciences “The origin and evolution of stars and galaxies”, program held by the Section for Physical sciences of RAS “Extended objects in the Universe”. This publication is based on work supported by Award No.RUP1–2687–NA–05 of the U.S. Civilian Research & Development Foundation (CRDF). In our study we used SIMBAD and ADS databases.

References

1. S. Kwok, 1993. *Ann. Rev. Astron. Astrophys.* 31, 63
2. T. Ueta, M. Meixner, and M. Bobrowsky, 2000. *Astrophys. J.* 528, 861
3. R.D. Oudmaijer and E.J. Bakker, 1994. *Mon. Not. R. Astron. Soc.* 271, 615
4. V.G. Klochkova, 1995. *Mon. Not. R. Astron. Soc.* 272, 710
5. V.G. Klochkova, 1998. *Bull. Spec. Astrophys. Obs.* 44, 5
6. L. Decin, H. van Winckel, C. Waelkens, and E.J. Bakker, 1998. *Astron. Astrophys.* 332, 928
7. V.E. Panchuk, V.G. Klochkova, I.D. Naidenov, 1999. Preprint *Spec. Astrophys. Obs.*, No.135,
8. V.E. Panchuk, N.E. Piskunov, V.G. Klochkova, et al., 2002. Preprint *Spec. Astrophys. Obs.*, Russ. No.169
9. V.G. Klochkova, S.V. Ermakov, V.E. Panchuk, et al., 1999. Preprint *Spec. Astrophys. Obs.*, No.137
10. V.E. Panchuk, V.G. Klochkova, and I.D. Naidenov, 1999. Preprint *Spec. Astrophys. Obs.*, No.139
11. V.E. Panchuk, M.V. Yushkin, and I.D. Naidenov, 2003. Preprint *Spec. Astrophys. Obs.*, No.179
12. M.V. Yushkin, V.G. Klochkova, 2005. Preprint *Spec. Astrophys. Obs.*, No.206
13. G.A. Galazutdinov, 1992. Preprint *Spec. Astrophys. Obs.*, No.192
14. E.J. Bakker, L.B.F.M. Waters, H.J.G.L.M. Lamers, et al., 1996. *Astron. Astrophys.* 310, 893
16. I.A. Crawford and M.J. Barlow, 2000. *Mon. Not. R. Astron. Soc.* 311, 370
15. A. L'ebre, N. Mauron, D. Gillet, and D. Barth'ès, 1996. *Astron. Astrophys.* 310, 923
17. E.J. Bakker, E.F. Dishoeck, L.B.F.M. Waters, and T. Schoenmaker, 1997. *Astron. Astrophys.* 323, 469
18. D. Barth'ès, A. L'ebre, D. Gillet, and N. Mauron, 2000. *Astron. Astrophys.* 359, 168
19. V.G. Klochkova, R. Szczerba, V.E. Panchuk, and K. Volk, 1999. *Astron. Astrophys.* 345, 905
20. V.G. Klochkova, R. Szczerba, and V. E. Panchuk, 2000. *Astron. Lett.* 26, 88
21. V. G. Klochkova, R. Szczerba, and V. E. Panchuk, 2000. *Astron. Lett.* 26, 439
22. V.G. Klochkova and E. L. Chentsov, 2004. *Astron. Rep.* 48, 301
23. Rao N. Kameswara, A. Goswami, and D.L. Lambert, 2002. *Mon. Not. R. Astron. Soc.* 334, 129
24. V.G. Klochkova, E.L. Chentsov, V. E. Panchuk, M.V. Yushkin, 2007. *Astrophys. Bull.* 62, 217
25. V.G. Klochkova, V.E. Panchuk, N.S. Tavolganskaya, and G. Zhao, 2006. *Astron. Rep.* 50, 232
26. S.R. Trammell, H.L. Dinerstein, R.W. Goodrich, 1994. *Astrophys. J.* 108, 984
27. M. Parthasarathy, P. Garcia Lario, and S.R. Pottasch, 1992. *Astron. Astrophys.* 264, 159
28. P. Mathias, D. Gillet, A. B. Fokin, et al., 2006. *Astron. Astrophys.* 457, 575
29. A. L'ebre and D. Gillet, 1991. *Astron. Astrophys.* 246, 490
30. G. Wallerstein, 2002. *Publ. Astron. Soc. Pac.* 114, 689
31. A.A. Ferro, 1984. *Publ. Astron. Soc. Pac.* 96, 641
32. L.B.F.M. Waters, C. Waelkens, M. Mayor, and N.R. Trams, 1993. *Astron. Astrophys.* 269, 242
33. C. Waelkens, H.J.G.L.M. Lamers, L.B.F.M. Waters, et al., 1991. *Astron. Astrophys.* 242, 433
34. H. van Winckel, C. Waelkens, and L.B.F.M. Waters, 1995 *Astron. Astrophys.* 293, L25
35. E.J. Bakker, D.L. Lambert, H. van Winckel, et al., 1998. *Astron. Astrophys.* 336, 263
36. A. L'ebre, A.B. Fokin, D. Barth'ès, et al., 2001. *Astrophys. Space Sci.* 265, 105
37. V. Bujarrabal, J. Alcolea, and P. Planesas, 1992. *Astron. Astrophys.* 257, 701

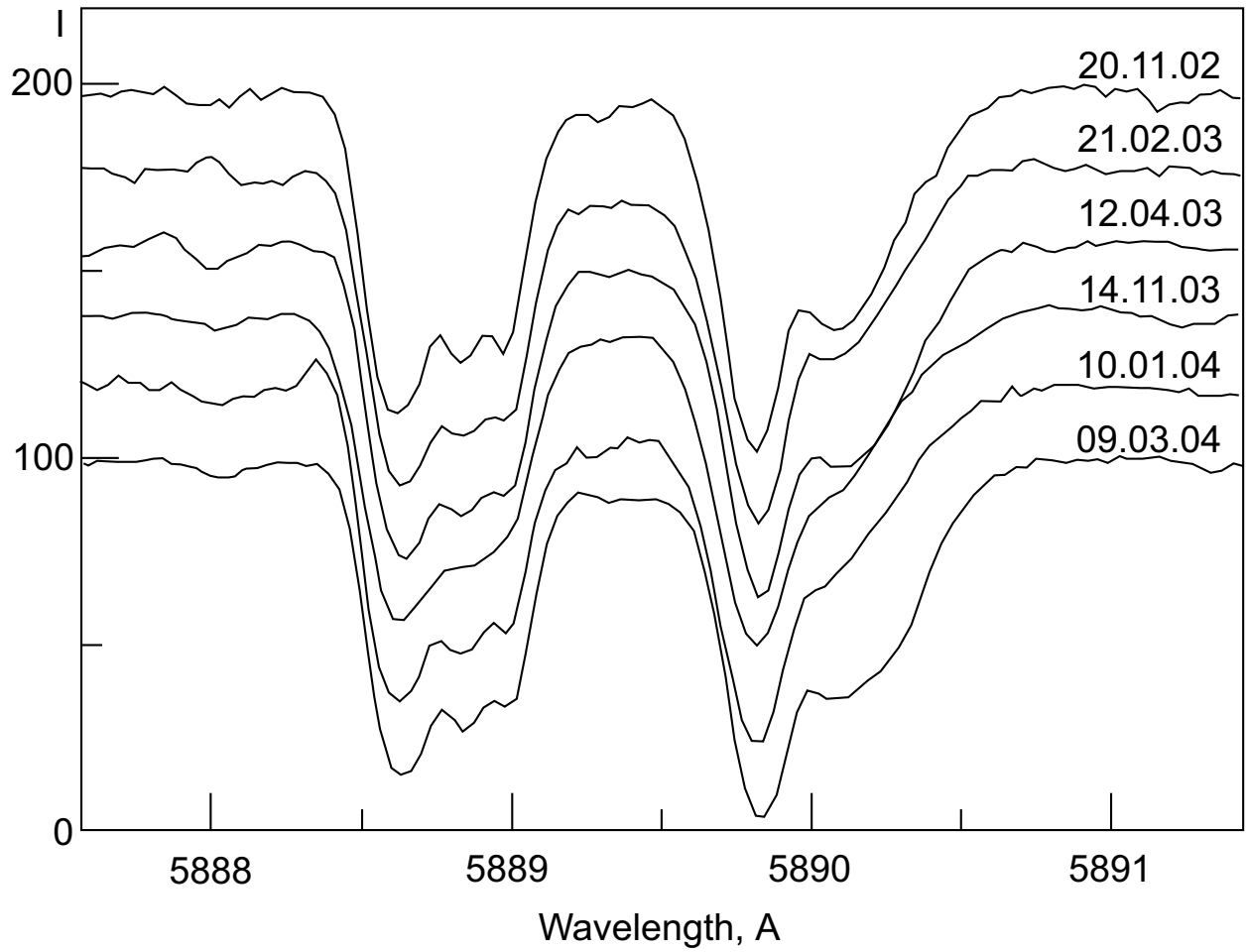


Figure 1. Spectral fragments containing the D2 NaI line for various observing dates

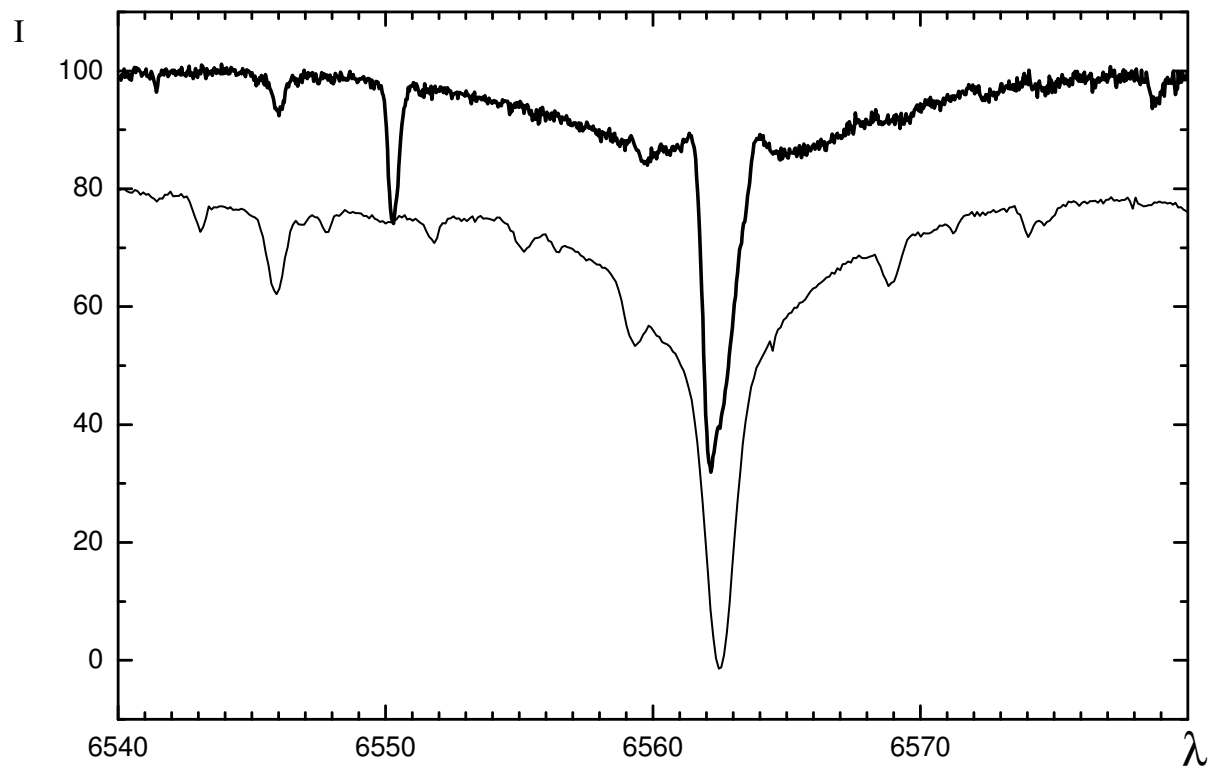


Figure 2. $H\alpha$ profile in the spectra of HD 56126 (top) and α Per (bottom).

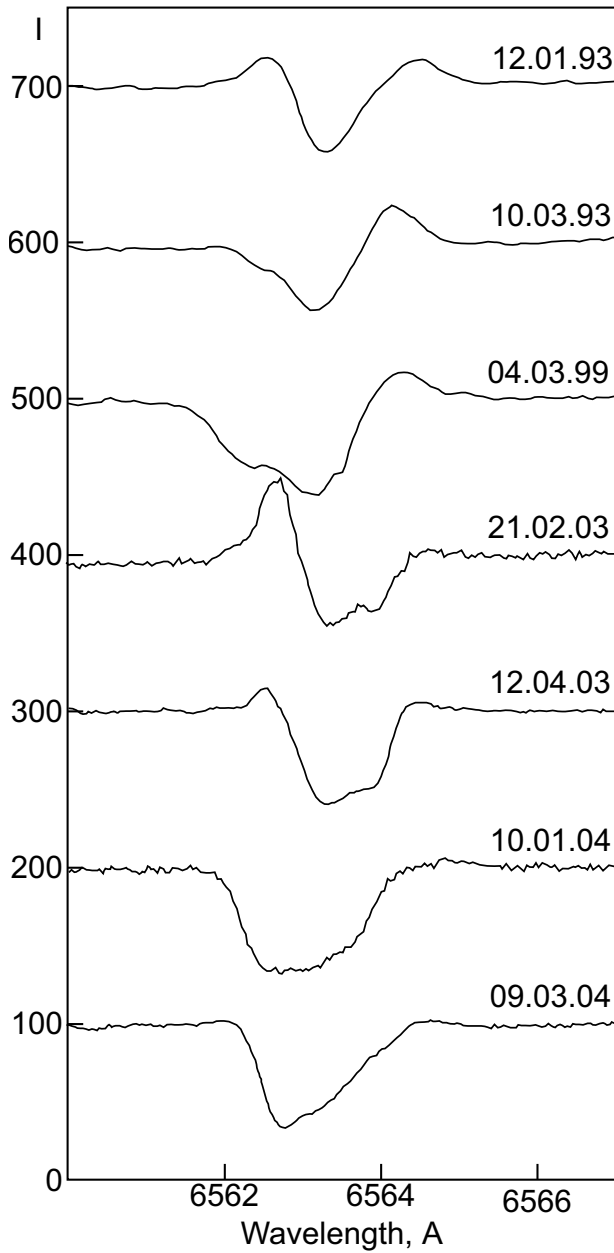


Figure 3. Central part of the H α profile in the spectra of HD 56126 obtained on different nights.

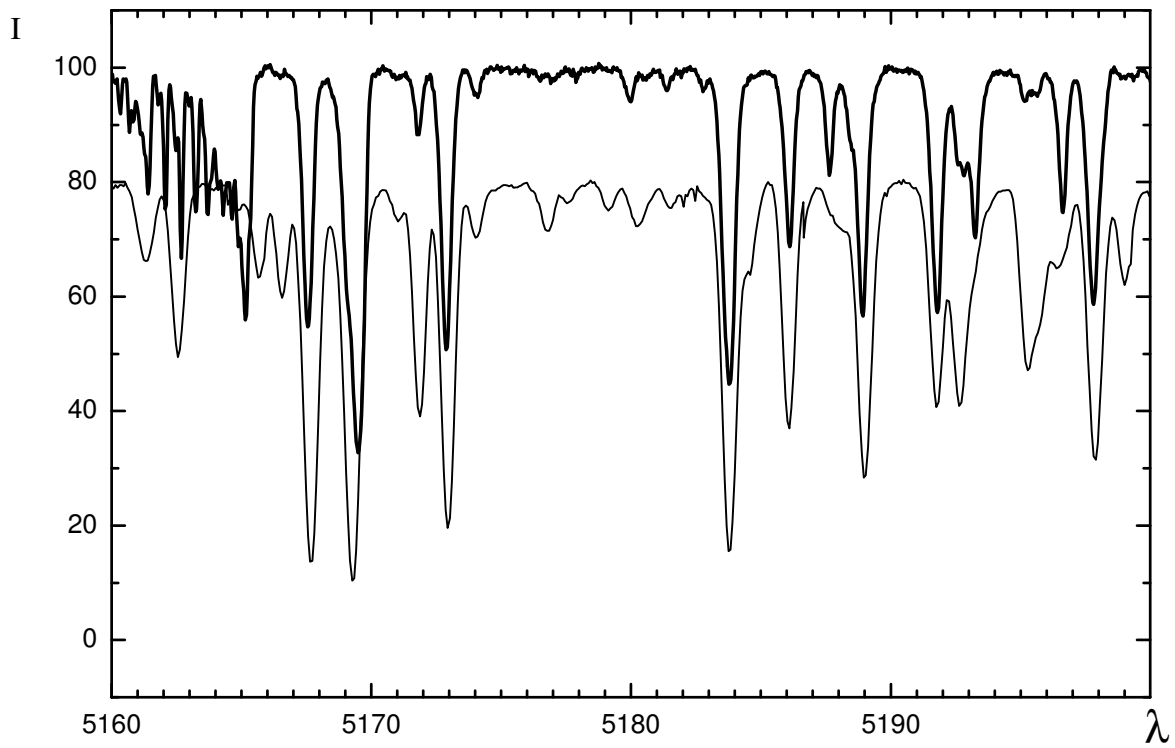


Figure 4. Fragment of the spectrum of HD 56126 with the Swan band 5165 Å of the C₂ molecule. For comparison, the same spectral fragment for α Per is presented below.

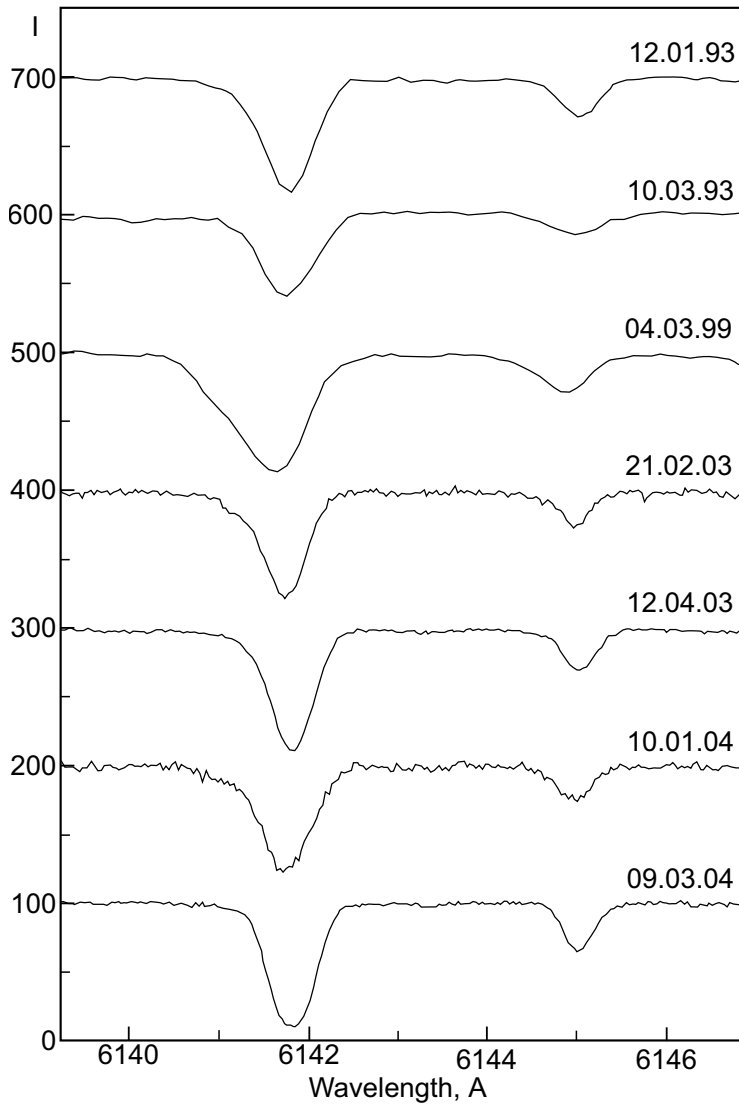


Figure 5. Variability of the BaII 6141 Å line profile in the spectrum of HD 56126.

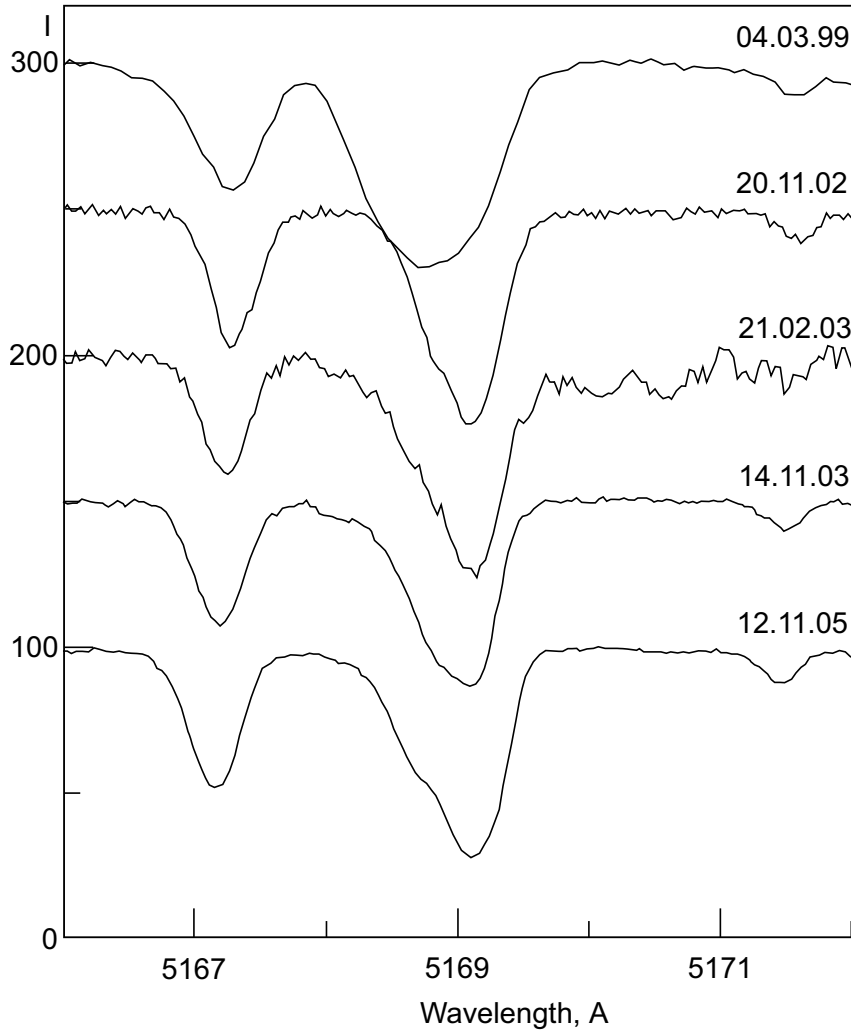


Figure 6. Variability of the FeII 5169 Å line profile in the spectrum of HD 56126.

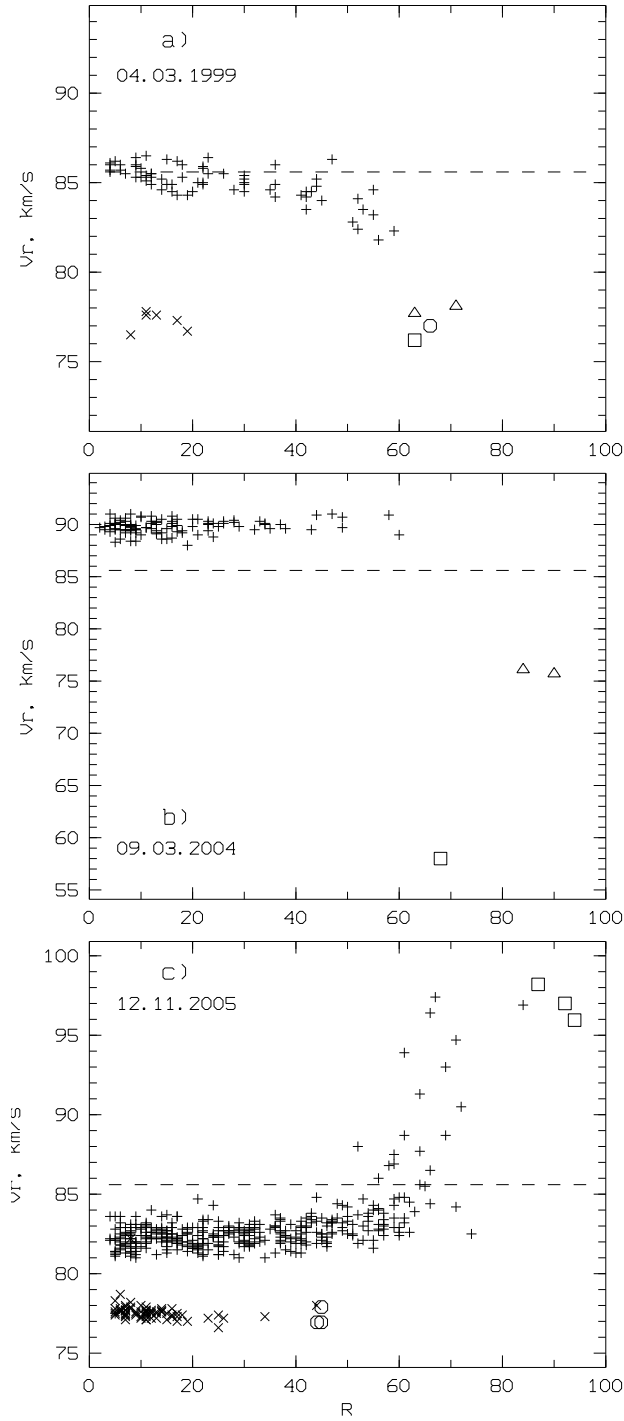


Figure 7. Dependence of the heliocentric radial velocity derived from the absorption core on its depth R in the spectrum of HD 56126 for various nights: (a) March 4, 1999, (b) March 9, 2004, (c) November 12, 2005. The dashed line indicates the systemic velocity. Each symbol denotes a particular type of spectral line: the pluses denote lines of metals; the daggers – C_2 lines; and the triangles, circle, and square – the main components of the D2 NaI, FeII(42) 5169 Å, and $H\alpha$ lines, respectively. In graph (c), the circles denote the secondary components of the FeII(42) lines, and the squares the $H\beta$, $H\gamma$, and $H\delta$ lines (top to bottom). The size of the symbols corresponds to the accuracy of the V_r measurements and the depth of the lines.